Diagonal forms of the translation operators in the fast multipole algorithm for scattering problems

Jussi Rahola
Helsinki University of Technology
Institute of Mathematics
Otakaari 1 M
FIN-02150 Espoo
Finland

Permanent address:
Center for Scientific Computing
P.O. Box 405
FIN-02101 Espoo
Finland
Jussi.Rahola@csc.fi

April 13, 1995

Submitted to BIT

AMS subject classifications: 65R20, 78A45

Key words: Integral equations, scattering, fast multipole method

Abstract

The integral equations of acoustic and electromagnetic scattering generate large dense systems of linear equations. These systems are efficiently solved with iterative methods where the matrix-vector multiplication is computed using a special fast method, such as the fast Fourier transform or the fast multipole method (FMM). In this paper, the so called diagonal forms of the translation operators for the fast multipole method are derived starting from integral representations of certain special functions. Error analysis of the FMM is given, considering both the truncation error of potential expansions and the errors from the use of numerical integration in the diagonal translation theorem. The implications of the error bounds on the FMM algorithm are discussed.

1 Introduction

The fast multipole method (FMM) developed by Greengard and Rokhlin is an efficient algorithm for the evaluation of potential and force fields in N-body simulations, where all pairwise interactions of N particles are computed. Traditional methods requite on the order of $\mathcal{O}(N^2)$ operations whereas FMM algorithms can achieve $\mathcal{O}(N)$ complexity ($\mathcal{O}(N \log N)$ complexity in scattering problems).

The fast multipole method is based on truncated potential expansions. The information on the potential of far-away sources is compressed to the first few coefficients of the potential expansions. The first applications of the FMM used the gravitational potential in celestial mechanics or the Coulombic potential in molecular dynamics [12].

The major computational task in the numerical solution of integral equations is the solution of dense systems of linear equations. When these systems are solved with iterative methods, most of the computing time is spent in the computation of the product of the coefficient matrix with a given vector. The FMM ideas were actually introduced by Rokhlin [23] in conjunction with the solution of integral equations, namely in the solution of a boundary value problem for the Laplace equation.

Scattering problems are elegantly cast as either surface or volume integral equations. Surface integral equations involve fewer degrees of freedom but for inhomogeneous scatterers or for particles with very irregular surfaces, volume integral equations are employed. The FMM was applied to a 2D acoustic scattering problem in [24] and to a 2D electromagnetic scattering problem in [8]. The fast Fourier transform can be used to compute the matrix-vector product in volume integral equations (see e.g. [26]). The FMM gives greatest benefit with surface integral equations but also with volume integral equations for porous irregular particles.

In the FMM algorithm the heaviest operations are the translation of the origin of the potential expansions and the conversion of the multipole expansion to a local expansion. It was shown by Rokhlin [25] that the translations of the potential expansions can be expressed as diagonal operators in Fourier space. The diagonal translation theory was summarized and extended by Epton and Bembart [9]. These two works considered the expansion of the Green's function for the scattering problems. Coifman, Rokhlin, and Wandzura also showed the actual connection to the scattering integral equation [6].

In this article we shall present a simplified derivation of the diagonal forms for the translation operators, along the lines given in [6]. Our approach is related to the "fast multipole method without multipoles" approach by Anderson [2]. The diagonal forms of the translation operators are derived from expansions and integral representations of the Green's functions for the acoustic and electromagnetic scattering problems. The Green's function for the acoustic scattering problem (scalar Helmholtz equation) is equivalent to the potential of an oscillating electric dipole. Similarly, the Green's function for the electromagnetic case (vector Helmholtz equation) is equivalent to the electric field of a dipole.

In Section 2 we shall introduce the expansions of the Green's functions and the various special functions. Several useful identities are derived. The diagonal forms

of the translation operators for the FMM algorithm are presented in Section 3. The integral representations of the potential are employed while the integrals are approximated by numerical quadrature.

There are two sources of errors in the FMM algorithm. First, the infinite potential expansions are truncated to a finite degree. The second error source is the numerical quadrature in the diagonal forms. These two errors will be analysed in Section 4. Due to the complicated asymptotic behaviour of the Bessel functions, the error analysis is considerably more complicated than in the case of a gravitational or Coulombic potential.

Throughout this paper, we will work with the dipole potential and the electric field caused by a dipole. This is done mainly for clarity of exposition. We will also show how the scattering integral equation connects to this formalism. However, electric dipoles appear also directly in scattering computations. The discrete-dipole approximation (DDA) [20] approximates the particle as a collection of interacting electric dipoles. The numerical aspects of the DDA algorithm are discussed for example in [15, 22]. The iterative method called quasi-minimal residual method (QMR) [10] was found to be the most suitable for the problems. The DDA appears also when the volume scattering integral equation is discretized using piecewise constant basis functions and a collocation or point-matching technique is used [21]. In actual computations the use of the integral equation is preferred over the DDA, but the DDA may be a useful pedagogical device.

2 Special functions

In the fast multipole algorithm we use potential expansions of the dipole potential (or the Green's function) in terms of spherical Bessel functions, Legendre polynomials, and spherical harmonics. In this section we introduce the expansions and special functions.

The principal tool in the theory of the fast multipole method for 3-D scattering problems is the expansion ([1], 10.1.45 and 10.1.46)

$$\frac{e^{ik|\mathbf{x}+\mathbf{y}|}}{ik|\mathbf{x}+\mathbf{y}|} = h_0^{(1)}(k|\mathbf{x}+\mathbf{y}|) = \sum_{l=0}^{\infty}(2l+1)(-1)^l h_l^{(1)}(kx) j_l(ky) P_l(\hat{\mathbf{x}}\cdot\hat{\mathbf{y}}), \qquad (1)$$

or equivalently

$$\frac{e^{ik|\mathbf{x}+\mathbf{y}|}}{ik|\mathbf{x}+\mathbf{y}|} = 4\pi \sum_{l=0}^{\infty}\sum_{m=-l}^{l}(-1)^l h_l^{(1)}(kx) j_l(ky)[Y_l^m(\hat{\mathbf{x}})]^* Y_l^m(\hat{\mathbf{y}}). \qquad (2)$$

We have denoted $x = |\mathbf{x}|$ and $\hat{\mathbf{x}} = \mathbf{x}/x$, the asterisk denotes complex conjugation, and k is the wave number. Moreover, we assumed that $x > y$. If $\hat{\mathbf{s}}$ is a unit vector in the direction given by θ, ϕ ($\hat{\mathbf{s}} = (\sin\theta\cos\phi, \sin\theta\sin\phi, \cos\theta)$), we use $Y_l^m(\hat{\mathbf{s}})$ as a synonym for $Y_l^m(\theta,\phi)$.

We use special functions as defined in Abramowitz and Stegun [1] and Arfken [3]. In addition to the spherical Bessel functions $j_l(x)$ and the spherical Hankel functions

of the first kind $h_l^{(1)}(x)$ we also use the spherical Neumann functions $n_l(x)$. These are defined in terms of the Bessel functions $J_l(x)$, Neumann functions $N_l(x)$, and the Hankel functions of the first kind $H_l^{(1)}(x)$ by

$$\begin{aligned} j_l(x) &= \sqrt{\frac{\pi}{2x}} J_{l+\frac{1}{2}}(x), && (3) \\ n_l(x) &= \sqrt{\frac{\pi}{2x}} N_{l+\frac{1}{2}}(x), && (4) \\ h_l^{(1)}(x) &= \sqrt{\frac{\pi}{2x}} H_{l+\frac{1}{2}}^{(1)}(x). && (5) \end{aligned}$$

Note that

$$H_l^{(1)}(x) = J_l(x) + iN_l(x), \tag{6}$$

giving

$$h_l^{(1)}(x) = j_l(x) + in_l(x). \tag{7}$$

We shall refer to the functions $J_l(x)$, $N_l(x)$, and $H_l^{(1)}(x)$ collectively as Bessel functions and to the functions $j_l(x)$, $n_l(x)$, and $h_l^{(1)}(x)$ as spherical Bessel functions. The Bessel and spherical Bessel functions appear when the Helmholtz equation is solved in circular cylindrical coordinates and in the spherical polar coordinates, respectively.

The Legendre polynomials are defined by

$$P_l(x) = \frac{1}{2^l l!} \frac{d^l}{dx^l} (x^2 - 1)^l. \tag{8}$$

The spherical harmonics are defined by

$$Y_l^m(\theta, \phi) = (-1)^m \sqrt{\frac{(2l+1)}{4\pi} \frac{(l-m)!}{(l+m)!}} P_l^m(\cos\theta) e^{im\phi}, \tag{9}$$

where the associated Legendre functions are given by

$$\begin{aligned} P_l^m(x) &= (1-x^2)^{m/2} \frac{d^m}{dx^m} P_l(x), \quad m \geq 0, \\ P_l^{-m}(x) &= (-1)^m \frac{(l-m)!}{(l+m)!} P_l^m(x), \quad -m < 0. && (10) \end{aligned}$$

The spherical harmonics and Legendre polynomials are connected by the addition theorem

$$P_l(\hat{\mathbf{x}} \cdot \hat{\mathbf{y}}) = \frac{4\pi}{2l+1} \sum_{m=-l}^{l} [Y_l^m(\hat{\mathbf{x}})]^* Y_l^m(\hat{\mathbf{y}}), \tag{11}$$

which naturally establishes the equivalence of (1) and (2).

The spherical harmonics appear when the Helmholtz equations is solved by the separation of variables in spherical polar coordinates. Note that there are many normalization and sign conventions associated with the spherical harmonics. We use the

Condon-Shortley phase convention. Our normalization leads to the orthonormality relation

$$\int_{-\pi}^{\pi}\int_{0}^{\pi} Y_l^m(\theta,\phi)[Y_{l'}^{m'}(\theta,\phi)]^* \sin\theta \, d\theta \, d\phi = \delta_{mm'}\delta_{ll'}. \tag{12}$$

This can be put in a more compact form by using the element of solid angle (element of area on the unit sphere S_1) $d\omega_s = \sin\theta \, d\theta \, d\phi$:

$$\int_{S_1} Y_l^m(\hat{\mathbf{s}})[Y_{l'}^{m'}(\hat{\mathbf{s}})]^* \, d\omega_s = \delta_{mm'}\delta_{ll'}. \tag{13}$$

From Equations (13) and (11) we can derive an orthogonality relation for the Legendre polynomials:

$$\begin{aligned}
&\int_{S_1} P_l(\hat{\mathbf{y}}\cdot\hat{\mathbf{s}})P_{l'}(\hat{\mathbf{s}}\cdot\hat{\mathbf{x}}) \, d\omega_s = \\
&\quad \frac{4\pi}{2l+1}\frac{4\pi}{2l'+1}\sum_{m=-l}^{l}\sum_{m'=-l'}^{l'}\int_{S_1}[Y_l^m(\hat{\mathbf{y}})]^* Y_{l'}^{m'}(\hat{\mathbf{x}})[Y_{l'}^{m'}(\hat{\mathbf{s}})]^* Y_l^m(\hat{\mathbf{s}}) \, d\omega_s = \\
&\quad \delta_{ll'}\left(\frac{4\pi}{2l+1}\right)^2 \sum_{m=-l}^{l}[Y_l^m(\hat{\mathbf{x}})]^* Y_l^m(\hat{\mathbf{y}}) = \delta_{ll'}\frac{4\pi}{2l+1}P_l(\hat{\mathbf{x}}\cdot\hat{\mathbf{y}}).
\end{aligned} \tag{14}$$

The potential expansion (1) can be put in a form where the translation operators become diagonal. We first need the partial wave expansion of the plane wave ([1], 10.1.47)

$$e^{iz\cos\gamma} = \sum_{l=0}^{\infty}(2l+1)i^l j_l(z)P_l(\cos\gamma). \tag{15}$$

Using this expansion and Equation (14) we obtain

$$\begin{aligned}
\int_{S_1} e^{i\mathbf{y}\cdot\hat{\mathbf{s}}}P_l(\hat{\mathbf{s}}\cdot\hat{\mathbf{x}}) \, d\omega_s \;&=\; \sum_{l'=0}^{\infty}(2l'+1)i^{l'}j_{l'}(y)\int_{S_1} P_{l'}(\hat{\mathbf{s}}\cdot\hat{\mathbf{y}})P_l(\hat{\mathbf{s}}\cdot\hat{\mathbf{x}}) \, d\omega_s = \\
&\quad 4\pi i^l j_l(y)P_l(\hat{\mathbf{x}}\cdot\hat{\mathbf{y}}).
\end{aligned} \tag{16}$$

Combining the previous result with the potential expansion (1) we get

$$\frac{e^{ik|\mathbf{x}+\mathbf{y}|}}{ik|\mathbf{x}+\mathbf{y}|} = \frac{1}{4\pi}\sum_{l=0}^{\infty}(2l+1)i^l h_l^{(1)}(kx)\int_{S_1} e^{ik\mathbf{y}\cdot\hat{\mathbf{s}}}P_l(\hat{\mathbf{s}}\cdot\hat{\mathbf{x}}) \, d\omega_s. \tag{17}$$

This form will be the basis of our derivation of the diagonal translation theorem for multipole and local expansions.

Especially in the error analysis section we will be using dyads as introduced by Gibbs [11]. For an recent introduction to dyads, see Lindell [14]. The dyadic product of two vectors $\mathbf{a}$ and $\mathbf{b}$ is the dyad (or tensor) $\mathbf{ab}$. If a and b are the column vector representations of $\mathbf{a}$ and $\mathbf{b}$ in some basis, the dyad is represented by the matrix ab^T. The dyad is a linear mapping: the mapping $\mathbf{p} \to \mathbf{a}(\mathbf{b}\cdot\mathbf{p})$ can be written in dyadic notation as $(\mathbf{ab})\cdot\mathbf{p}$. The unit dyad is denoted by $\mathbf{1}$ (represented by the identity matrix), given in Cartesian coordinates by $\mathbf{ii}+\mathbf{jj}+\mathbf{kk}$. The dyadic $\nabla\nabla$ contains the second-order partial derivatives, so it is the Hessian matrix. Alternative notation for the operator $\nabla\nabla\cdot$ is **grad div**. It should not be confused with the Laplacian $\nabla^2 = \nabla\cdot\nabla =$ **div grad**.

3 Translation operators

The fast multipole algorithm is based on the manipulation of truncated potential expansions. In order to evaluate the potential of "particles" in group A at the locations of "particles" in group B, the multipole and local expansions are used. The multipole expansion of group A is valid when the origin of the expansion is near the particles and the evaluation point is far away. The local expansion of particles in group A is valid when the evaluation point is near the origin and the particles are far from the origin.

In the non-adaptive FMM algorithm [12] we need to form the multipole expansion from the particles, translate the expansion to another point, transform the multipole expansion to a local expansion, translate the local expansion, and finally evaluate the local expansions. In the adaptive FMM algorithm [5, 18] we also need to evaluate the potential directly from the multipole expansion and to form the local expansion directly from the particles.

A straightforward approach to the multipole expansions is to use the potential expansion (2): the multipole coefficients of a collection of N_{dip} dipoles are defined by

$$\mathbf{M}_{lm} = \sum_{i=1}^{N_{dip}} \mathbf{p}_i j_l(kr_i) \left[Y_l^m(\theta_i, \phi_i)\right]^* , \tag{18}$$

where k is the wave number, $\mathbf{p}_i$ is the dipole moment, and r_i, θ_i, and ϕ_i are the spherical coordinates of the dipole i at position $\mathbf{r}_i$. The multipole expansion of the potential in terms of the multipole coefficients is

$$\boldsymbol{\phi}(\mathbf{r}) = 4\pi \sum_{l=0}^{\infty} \sum_{m=-l}^{l} \mathbf{M}_{lm} h_l^{(1)}(kr) Y_l^m(\theta, \phi). \tag{19}$$

However, the translation operators for these types of multipole expansions are convolutions that are rather expensive to compute: if a p^2-term multipole expansion is used, its translation to another origin takes $\mathcal{O}(p^5)$ operations [9, 22].

Diagonal forms of translation operators for the Helmholtz equation were introduced by Rokhlin [24, 25, 6] and some of the results were presented in another framework by Epton and Dembart [9]. The basic idea is to work with essentially Fourier transformed quantities where the convolution (and also differentiation) become diagonal operators.

In numerical computation, the angle-dependent part of the multipole expansions is represented as discrete samples at the numerical quadrature points on the surface of the unit sphere. The potential can be recovered using numerical integration.

Here we will develop the multipole translation theory using only the expansion (17). Our approach simplifies and clarifies the results given in references [25] and [9].

In the sequel we will first consider the potential expansions of the vector potential of a dipole. Then we will work directly with the electromagnetic field.

3.1 The vector potential of a dipole

Assume that we have a collection of dipoles at positions $\mathbf{r}_j$ with dipole moments $\mathbf{p}_j$. Suppose that these are located near points $\mathbf{a}$ and $\mathbf{b}$. Furthermore, suppose that we need to evaluate the potential generated by the dipoles at point $\mathbf{r}$ near points $\mathbf{c}$ and $\mathbf{d}$ (see Figure 1). At first, let us write the vector $\mathbf{r}-\mathbf{r}_j$ as $\mathbf{r}-\mathbf{c}+\mathbf{c}-\mathbf{a}+\mathbf{a}-\mathbf{r}_j$. Let us denote $\mathbf{x}=\mathbf{c}-\mathbf{a}$ and $\mathbf{y}=\mathbf{r}-\mathbf{c}+\mathbf{a}-\mathbf{r}_j$, giving $\mathbf{r}-\mathbf{r}_j=\mathbf{x}+\mathbf{y}$. We furthermore assume that $|\mathbf{x}|>|\mathbf{y}|$ for all $\mathbf{r}_j$. Now we can put these into Equation (17) obtaining

$$\frac{e^{ik|\mathbf{r}-\mathbf{r}_j|}}{ik|\mathbf{r}-\mathbf{r}_j|}=\frac{1}{4\pi}\sum_{l=0}^{\infty}(2l+1)i^l h_l^{(1)}(k|\mathbf{c}-\mathbf{a}|)\int_{S_1} e^{ik(\mathbf{r}-\mathbf{c})\cdot\hat{\mathbf{s}}}P_l(\hat{\mathbf{s}}\cdot\frac{\mathbf{c}-\mathbf{a}}{|\mathbf{c}-\mathbf{a}|})e^{ik(\mathbf{a}-\mathbf{r}_j)\cdot\hat{\mathbf{s}}}\,d\omega_s. \tag{20}$$

If the sum over l is truncated, we can exchange the summation and integration and define a function M_L

$$M_L(\hat{\mathbf{s}},\mathbf{r})=\sum_{l=0}^{L}(2l+1)i^l h_l^{(1)}(kr)P_l(\hat{\mathbf{s}}\cdot\hat{\mathbf{r}}), \tag{21}$$

resulting in

$$\frac{e^{ik|\mathbf{r}-\mathbf{r}_j|}}{ik|\mathbf{r}-\mathbf{r}_j|}=\lim_{L\to\infty}\frac{1}{4\pi}\int_{S_1} e^{ik(\mathbf{r}-\mathbf{c})\cdot\hat{\mathbf{s}}}M_L(\hat{\mathbf{s}},\mathbf{c}-\mathbf{a})e^{ik(\mathbf{a}-\mathbf{r}_j)\cdot\hat{\mathbf{s}}}\,d\omega_s. \tag{22}$$

The vector potential generated by an oscillating electric dipole with a dipole moment $\mathbf{p}_j$ is [13]

$$\mathbf{A}_j(\mathbf{r})=-ik\mathbf{p}_j\frac{e^{ik|\mathbf{r}-\mathbf{r}_j|}}{|\mathbf{r}-\mathbf{r}_j|}. \tag{23}$$

Using (22), we define the truncated potential expansion

$$\mathbf{A}_{j,L}(\mathbf{r})=\frac{k^2}{4\pi}\int_{S_1} e^{ik(\mathbf{r}-\mathbf{c})\cdot\hat{\mathbf{s}}}M_L(\hat{\mathbf{s}},\mathbf{c}-\mathbf{a})e^{ik(\mathbf{a}-\mathbf{r}_j)\cdot\hat{\mathbf{s}}}\mathbf{p}_j\,d\omega_s, \tag{24}$$

for which $\lim_{L\to\infty}\mathbf{A}_{j,L}(\mathbf{r})=\mathbf{A}_j(\mathbf{r})$.

For a collection of N_{dip} dipoles near point $\mathbf{a}$, if we substitute $\mathbf{r}$ for $\mathbf{c}$ in (24) and sum over the dipoles, we get

$$\mathbf{A}_L(\mathbf{r})=\frac{k^2}{4\pi}\int_{S_1} M_L(\hat{\mathbf{s}},\mathbf{r}-\mathbf{a})\sum_{j=1}^{N_{dip}} e^{ik(\mathbf{a}-\mathbf{r}_j)\cdot\hat{\mathbf{s}}}\mathbf{p}_j\,d\omega_s. \tag{25}$$

On the other hand, substituting $\mathbf{r}_j$ for $\mathbf{a}$ in (24) and summing over the dipoles, we obtain

$$\mathbf{A}_L(\mathbf{r})=\frac{k^2}{4\pi}\int_{S_1} e^{ik(\mathbf{r}-\mathbf{c})\cdot\hat{\mathbf{s}}}\sum_{j=1}^{N_{dip}} M_L(\hat{\mathbf{s}},\mathbf{c}-\mathbf{r}_j)\mathbf{p}_j\,d\omega_s. \tag{26}$$

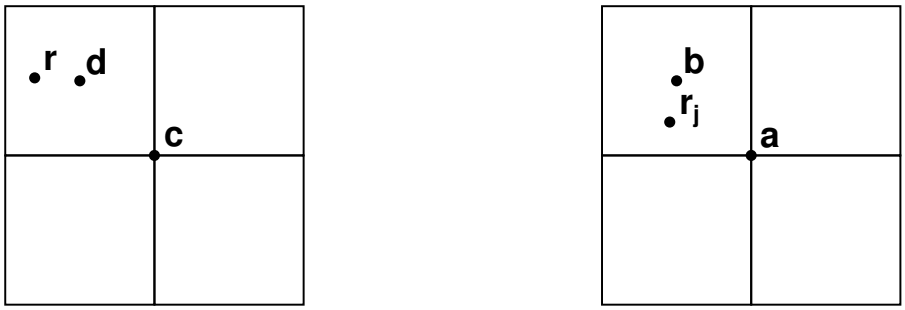

Figure 1: The dipole is at position $\mathbf{r}_j$ and its potential is evaluated at position $\mathbf{r}$. In the FMM algorithm the far-field signature function of the dipole centered at the points $\mathbf{a}$ and $\mathbf{b}$ is constructed. The near-field signature function centered at points $\mathbf{c}$ and $\mathbf{d}$ is constructed.

Now we can define the far-field signature function $\mathbf{F}_{\mathbf{a}}(\hat{\mathbf{s}})$ and the near-field signature function $\mathbf{N}_{\mathbf{c},L}(\hat{\mathbf{s}})$ of a collection of dipoles by

$$\mathbf{F}_{\mathbf{a}}(\hat{\mathbf{s}}) = \sum_{j=1}^{N_{dip}} e^{ik(\mathbf{a}-\mathbf{r}_j)\cdot\hat{\mathbf{s}}}\mathbf{p}_j, \tag{27}$$

$$\mathbf{N}_{\mathbf{c},L}(\hat{\mathbf{s}}) = \sum_{j=1}^{N_{dip}} M_L(\hat{\mathbf{s}}, \mathbf{c}-\mathbf{r}_j)\mathbf{p}_j. \tag{28}$$

Note that in the numerical implementation these are represented on a finite set of points on the unit sphere. The reconstruction formulas (25) and (26) now read

$$\mathbf{A}_L(\mathbf{r}) = \frac{k^2}{4\pi}\int_{S_1} M_L(\hat{\mathbf{s}}, \mathbf{r}-\mathbf{a})\mathbf{F}_{\mathbf{a}}(\hat{\mathbf{s}})\, d\omega_s. \tag{29}$$

and

$$\mathbf{A}_L(\mathbf{r}) = \frac{k^2}{4\pi}\int_{S_1} e^{ik(\mathbf{r}-\mathbf{c})\cdot\hat{\mathbf{s}}}\mathbf{N}_{\mathbf{c},L}(\hat{\mathbf{s}})\, d\omega_s. \tag{30}$$

In practical calculations, the dipole potential is retrieved using numerical integration on the points that were used to represent the far-field and near-field signature functions (see (76)).

Inserting Equation (27) into (24) and comparing this with (30) allows us to relate the far-field and near-field representations by

$$\mathbf{N}_{\mathbf{c},L}(\hat{\mathbf{s}}) = M_L(\hat{\mathbf{s}}, \mathbf{c}-\mathbf{a})\mathbf{F}_{\mathbf{a}}(\hat{\mathbf{s}}) + g(\hat{\mathbf{s}}). \tag{31}$$

where $g(\hat{\mathbf{s}})$ is any function such that $\int_{S_1} e^{ik(\mathbf{r}-\mathbf{c})\cdot\hat{\mathbf{s}}} g(\hat{\mathbf{s}})\, d\omega_s = 0$. In the sequel we set $g(\hat{\mathbf{s}}) = 0$.

Furthermore, we can find the translation formulas for $\mathbf{F}_{\mathbf{a}}(\hat{\mathbf{s}})$ and $\mathbf{N}_{\mathbf{c},L}(\hat{\mathbf{s}})$ from looking at (24). Put $\mathbf{a}-\mathbf{r}_j = \mathbf{a}-\mathbf{b}+\mathbf{b}-\mathbf{r}_j$ in Equation (27), giving

$$\mathbf{F}_{\mathbf{a}}(\hat{\mathbf{s}}) = e^{ik(\mathbf{a}-\mathbf{b})\cdot\hat{\mathbf{s}}}\mathbf{F}_{\mathbf{b}}(\hat{\mathbf{s}}). \tag{32}$$

Similarly, write $\mathbf{r}-\mathbf{c}=\mathbf{r}-\mathbf{d}+\mathbf{d}-\mathbf{c}$ in Equation (30), giving

$$\mathbf{A}_L(\mathbf{r}) = \frac{k^2}{4\pi}\int_{S_1} e^{ik(\mathbf{r}-\mathbf{d})\cdot\hat{\mathbf{s}}} e^{ik(\mathbf{d}-\mathbf{c})\cdot\hat{\mathbf{s}}} \mathbf{N}_{\mathbf{c},L}(\hat{\mathbf{s}})\, d\omega_s, \tag{33}$$

which allows us to define

$$\mathbf{N}_{\mathbf{d},L}(\hat{\mathbf{s}}) = e^{ik(\mathbf{d}-\mathbf{c})\cdot\hat{\mathbf{s}}}\mathbf{N}_{\mathbf{c},L}(\hat{\mathbf{s}}). \tag{34}$$

Note that here we have set $g(\hat{\mathbf{s}})=0$.

Rokhlin together with Epton and Dembart [25, 9] define the far-field signature function of a potential ϕ by

$$\hat{\phi}_{\mathbf{a}}(\hat{\mathbf{s}}) = \lim_{r\to\infty}\left[\phi(\mathbf{a}+r\hat{\mathbf{s}})e^{-ikr}kr\right]. \tag{35}$$

Our far-field signature function (27) is equivalent (except for scaling) to this definition.

3.2 The electric field of a dipole

With the help of the diagonal translation theorem, working directly with the electric field of a dipole is no more difficult than working with the vector potential of a dipole. This is essentially due to use of Fourier transformed quantities, where the differentiation can be replaced by a diagonal operation.

The electric field caused by a dipole is given by [13]

$$\mathbf{E}_j(\mathbf{r}) = \frac{i}{k}\nabla\times(\nabla\times\mathbf{A}_j(\mathbf{r})) = (\nabla\nabla + k^2\mathbf{1})\frac{e^{ik|\mathbf{r}-\mathbf{r}_j|}}{|\mathbf{r}-\mathbf{r}_j|}\cdot\mathbf{p}_j. \tag{36}$$

Note the use of the dyad $\nabla\nabla$. Substituting (24) for $\mathbf{A}_j$ we can move the differentiation under the integral, where the differentiation is essentially of the form

$$\nabla\times\nabla\times f(\mathbf{r})\mathbf{p}_j = \nabla\nabla f(\mathbf{r})\cdot\mathbf{p}_j - \nabla^2 f(\mathbf{r})\mathbf{p}_j, \tag{37}$$

where $f(\mathbf{r}) = e^{ik(\mathbf{r}-\mathbf{c})\cdot\hat{\mathbf{s}}}$. Writing out the derivatives we get

$$\nabla\times\nabla\times e^{ik(\mathbf{r}-\mathbf{c})\cdot\hat{\mathbf{s}}}\mathbf{p}_j = k^2 e^{ik(\mathbf{r}-\mathbf{c})\cdot\hat{\mathbf{s}}}(\mathbf{p}_j - (\mathbf{p}_j\cdot\hat{\mathbf{s}})\hat{\mathbf{s}}). \tag{38}$$

For the electric field we thus get

$$\mathbf{E}_j(\mathbf{r}) = \lim_{L\to\infty}\frac{k^3 i}{4\pi}\int_{S_1} e^{ik(\mathbf{r}-\mathbf{c})\cdot\hat{\mathbf{s}}} M_L(\hat{\mathbf{s}},\mathbf{c}-\mathbf{a}) e^{ik(\mathbf{a}-\mathbf{r}_j)\cdot\hat{\mathbf{s}}}(\mathbf{p}_j - (\mathbf{p}_j\cdot\hat{\mathbf{s}})\hat{\mathbf{s}})\, d\omega_s. \tag{39}$$

This equation will be the basis for the theory of the far-field forms and their translation formulas for the electric field.

As in the case of the vector potential of the dipole, a completely analogous procedure allows us to write the far-field and near-field signature functions and their translation theorems, resulting in the following theorem.

Theorem 1 *The far-field signature function* $\mathbf{F}_{\mathbf{a}}(\hat{\mathbf{s}})$ *and the near-field signature function* $\mathbf{N}_{\mathbf{c},L}(\hat{\mathbf{s}})$ *of a collection of dipoles are defined by*

$$\mathbf{F}_{\mathbf{a}}(\hat{\mathbf{s}}) = \sum_{j=1}^{N_{dip}} e^{ik(\mathbf{a}-\mathbf{r}_j)\cdot\hat{\mathbf{s}}}(\mathbf{p}_j - (\mathbf{p}_j\cdot\hat{\mathbf{s}})\hat{\mathbf{s}}), \tag{40}$$

$$\mathbf{N}_{\mathbf{c},L}(\hat{\mathbf{s}}) = \sum_{j=1}^{N_{dip}} M_L(\hat{\mathbf{s}}, \mathbf{c}-\mathbf{r}_j)(\mathbf{p}_j - (\mathbf{p}_j\cdot\hat{\mathbf{s}})\hat{\mathbf{s}}). \tag{41}$$

The L*-term approximation to the electric field at position* r *is given by*

$$\mathbf{E}_L(\mathbf{r}) = \frac{k^3 i}{4\pi}\int_{S_1} M_L(\hat{\mathbf{s}}, \mathbf{r}-\mathbf{a})\mathbf{F}_{\mathbf{a}}(\hat{\mathbf{s}})\, d\omega_s \tag{42}$$

and

$$\mathbf{E}_L(\mathbf{r}) = \frac{k^3 i}{4\pi}\int_{S_1} e^{ik(\mathbf{r}-\mathbf{c})\cdot\hat{\mathbf{s}}}\mathbf{N}_{\mathbf{c},L}(\hat{\mathbf{s}})\, d\omega_s. \tag{43}$$

The far-field and near-field signature functions are related by

$$\mathbf{N}_{\mathbf{c},L}(\hat{\mathbf{s}}) = M_L(\hat{\mathbf{s}}, \mathbf{c}-\mathbf{a})\mathbf{F}_{\mathbf{a}}(\hat{\mathbf{s}}). \tag{44}$$

The translation formulas for $\mathbf{F}_{\mathbf{a}}(\hat{\mathbf{s}})$ *and* $\mathbf{N}_{\mathbf{c},L}(\hat{\mathbf{s}})$ *are given by*

$$\mathbf{F}_{\mathbf{a}}(\hat{\mathbf{s}}) = e^{ik(\mathbf{a}-\mathbf{b})\cdot\hat{\mathbf{s}}}\mathbf{F}_{\mathbf{b}}(\hat{\mathbf{s}}) \tag{45}$$

and

$$\mathbf{N}_{\mathbf{d},L}(\hat{\mathbf{s}}) = e^{ik(\mathbf{d}-\mathbf{c})\cdot\hat{\mathbf{s}}}\mathbf{N}_{\mathbf{c},L}(\hat{\mathbf{s}}). \tag{46}$$

3.3 Integral equation

In this subsection we move over to the scattering integral equation, and reformulate some of the results given in [6]. Our formulation is that of a volume integral equation, a surface integral equation is handled similarly.

The electric field inside a body occupying the space V is given by the integral equation [4]

$$\mathbf{E}(\mathbf{r}) = \mathbf{E}_{\text{inc}}(\mathbf{r}) + \int_V (m(\mathbf{r}')^2 - 1)\mathbf{G}(\mathbf{r},\mathbf{r}')\cdot\mathbf{E}(\mathbf{r}')\, d^3\mathbf{r}', \tag{47}$$

where $\mathbf{G}$ is the dyadic Green's function

$$\mathbf{G}(\mathbf{r},\mathbf{r}') = \left(k^2\mathbf{1} + \nabla\nabla\right) g(|\mathbf{r}-\mathbf{r}'|) \tag{48}$$

and

$$g(r) = \frac{e^{-ikr}}{4\pi r}. \tag{49}$$

Here $r = |\mathbf{r} - \mathbf{r}'|$, k is the wave number, $m(\mathbf{r})$ is the refractive index, and $\mathbf{E}_{\text{inc}}(\mathbf{r})$ is the incident field. To discretize this we expand the electric field in the basis functions $\mathbf{h}_i(\mathbf{r})$ that are zero outside of volume V_i:

$$\mathbf{E}(\mathbf{r}) = \sum_{i=1}^{N} z_i \mathbf{h}_i(\mathbf{r}). \tag{50}$$

The Galerkin method (or the method of moments) gives the system of linear equations $Az = b$, where z contains the unknown expansion coefficients and b is given by integrals over the basis functions and the incident field. The elements of the coefficient matrix are

$$A_{ij} = \int_{V_j} \int_{V_i} (m(\mathbf{r}')^2 - 1)[\mathbf{h}_i(\mathbf{r})]^* \cdot \mathbf{G}(\mathbf{r}, \mathbf{r}') \cdot \mathbf{h}_j(\mathbf{r}') \, d^3\mathbf{r} \, d^3\mathbf{r}'. \tag{51}$$

If iterative methods are used to solve the system of linear equations, the coefficient matrix need not be formed. During the solution procedure, the iterative method produces a guess for the unknown z. Using this we can compute the matrix-vector product and based on its value the iterative method adjusts the value of z.

The fast multipole method comes in like this: suppose that nearby basis functions are grouped into sets $W(l)$. We would like to compute the combined effect of basis functions in a set $W(l)$ (center $\mathbf{c}_l$) on those in a set $W(m)$ (center $\mathbf{c}_m$). Utilizing the Green's function expansion similar to (39), we define the far-field signature function

$$\mathbf{F}_{\mathbf{c}_l}(\hat{\mathbf{s}}) = \sum_{j \in W(l)} z_j \int_{V_j} e^{ik(\mathbf{c}_l - \mathbf{r}') \cdot \hat{\mathbf{s}}} (m(\mathbf{r}')^2 - 1)(\mathbf{h}_j(\mathbf{r}') - (\mathbf{h}_j(\mathbf{r}') \cdot \hat{\mathbf{s}})\hat{\mathbf{s}}) \, d^3\mathbf{r}'. \tag{52}$$

This is translated to a near-field signature function by

$$\mathbf{N}_{\mathbf{c}_m, L}(\hat{\mathbf{s}}) = M_L(\hat{\mathbf{s}}, \mathbf{c}_m - \mathbf{c}_l)\mathbf{F}_{\mathbf{c}_l}(\hat{\mathbf{s}}). \tag{53}$$

The value of the matrix-vector product corresponding to the interaction of a basis function $\mathbf{h}_i$ in set $W(m)$ with all the basis functions in set $W(l)$ is given by

$$\sum_{j \in W(l)} A_{ij} z_j = \frac{k^3 i}{(4\pi)^2} \int_{S_1} \int_{V_i} e^{ik(\mathbf{r} - \mathbf{c}_m) \cdot \hat{\mathbf{s}}} [\mathbf{h}_i(\mathbf{r})]^* \cdot \mathbf{N}_{\mathbf{c}_m, L}(\hat{\mathbf{s}}) \, d^3\mathbf{r} \, d\omega_s. \tag{54}$$

The other translation operators are defined accordingly.

4 Error analysis

Two kinds of errors are introduced in the FMM calculations. First, the infinite sum over l in (1) and related expansions is truncated. Moreover, the integrals appearing in, e.g., (24) are computed numerically resulting in discretization error. These errors will be analyzed in this section, first for the dipole potential and then for the electric field.

4.1 Error for the dipole potential

The infinite potential expansion of the dipole potential

$$\mathbf{A}_j(\mathbf{r}) = -ik\frac{e^{ik|\mathbf{r}-\mathbf{r}_j|}}{|\mathbf{r}-\mathbf{r}_j|} = -ik\frac{e^{ik|\mathbf{x}+\mathbf{y}|}}{|\mathbf{x}+\mathbf{y}|} = k^2\sum_{l=0}^{\infty}(2l+1)(-1)^l h_l^{(1)}(kx)j_l(ky)P_l(\hat{\mathbf{x}}\cdot\hat{\mathbf{y}}), \tag{55}$$

has to be truncated to a finite number of terms, say L terms. The vectors $\mathbf{x}$ and $\mathbf{y}$ are defined in Section 3.1. In the computations we use the expansion

$$-ik\frac{e^{ik|\mathbf{x}+\mathbf{y}|}}{|\mathbf{x}+\mathbf{y}|} = \frac{k^2}{4\pi}\sum_{l=0}^{\infty}(2l+1)i^l h_l^{(1)}(kx)\int_{S_1} e^{ik\mathbf{y}\cdot\hat{\mathbf{s}}}P_l(\hat{\mathbf{s}}\cdot\hat{\mathbf{x}})\,d\omega_s \tag{56}$$

and utilize the sum M_L from Equation (21). Because for a fixed x, the absolute value of $h_l^{(1)}(x)$ grows without limit as l grows, the sum in M_L does not converge. By the use of Equation (16), (56) reduces to (55) so that in exact arithmetic, the growth of $h_l^{(1)}(x)$ in (56) is implicitly balanced by the decay of the functions $j_l(y)$. However, because of numerical quadrature, the functions $j_l(y)$ appear only to a finite degree, thus reducing the number of terms in M_L that can be used. This will be analysed in more detail later.

Define the absolute value of the truncation error by

$$\begin{aligned}\epsilon_T &= \left|-ik\frac{e^{ik|\mathbf{x}+\mathbf{y}|}}{|\mathbf{x}+\mathbf{y}|} - k^2\sum_{l=0}^{L}(2l+1)(-1)^l h_l^{(1)}(kx)j_l(ky)P_l(\hat{\mathbf{x}}\cdot\hat{\mathbf{y}})\right| \\ &= \left|k^2\sum_{l=L+1}^{\infty}(2l+1)(-1)^l h_l^{(1)}(kx)j_l(ky)P_l(\hat{\mathbf{x}}\cdot\hat{\mathbf{y}})\right|.\end{aligned} \tag{57}$$

In order to approximate the truncation error, we need to consider the asymptotic behaviour of the spherical Bessel functions. The following formulae are exact:

$$j_l(x) = \frac{(2x)^l l!}{(2l+1)!}\,{}_0F_1(l+3/2, -x^2/4), \tag{58}$$

$$n_l(x) = -\frac{(2l-1)!}{x^2(2x)^{l-1}(l-1)!}\,{}_0F_1(-l+1/2, -x^2/4), \tag{59}$$

where ${}_0F_1(n,z)$ is the degenerate hypergeometric function defined by

$$\begin{aligned}{}_0F_1(n,z) &= \sum_{m=0}^{\infty}\frac{z^m}{m!(n)_m}, \\ (n)_0 &= 1, \\ (n)_m &= n(n+1)(n+2)\cdots(n+m-1).\end{aligned} \tag{60}$$

The factorials in the formula for Bessel functions can be approximated using Stirling's formula:

$$j_l(x) \sim \frac{1}{2l+1}\sqrt{\frac{e}{2}}\left(\frac{ex}{2l+1}\right)^l {}_0F_1(l+3/2,-x^2/4), \tag{61}$$

$$n_l(x) \sim -\frac{1}{x}\sqrt{\frac{2}{e}}\left(\frac{ex}{2l+1}\right)^{-l} {}_0F_1(-l+1/2,-x^2/4), \tag{62}$$

The hypergeometric functions can be approximated by ${}_0F_1(l+3/2,-x^2/4) \sim e^{-x^2/4l}$ and ${}_0F_1(-l+1/2,-x^2/4) \sim e^{x^2/4l}$. The latter approximation is valid only if $l > x$. Thus the asymptotic behaviour of the spherical Bessel functions is given by

$$j_l(x) \sim \frac{1}{2l+1}\sqrt{\frac{e}{2}}\left(\frac{ex}{2l+1}\right)^l e^{-x^2/4l}, \tag{63}$$

$$n_l(x) \sim -\frac{1}{x}\sqrt{\frac{2}{e}}\left(\frac{ex}{2l+1}\right)^{-l} e^{x^2/4l}. \tag{64}$$

These asymptotic expressions are valid only if $l > x$. After this point, the Bessel function $j_l(x)$ goes rapidly to zero, while the function $n_l(x)$ grows rapidly towards $-\infty$. Clearly, when $l > x$ the asymptotic behaviour of $h_l^{(1)}$ is essentially the same as the behaviour of function $n_l(x)$. To facilitate the error analysis, we have to replace the exponential term by some suitable constant in many places.

The analysis of the truncation error is gathered in the following result, which follows by inserting the asymptotic expressions of the spherical Bessel functions into (57).

Lemma 1 *For each k and x, there exists a constant C_1 such that the truncation error of the dipole potential is bounded by*

$$\epsilon_T \leq \frac{kC_1}{(x-y)}\left(\frac{y}{x}\right)^{L+1}, \tag{65}$$

where L is the number of terms in the truncated expansion, $x > y$, and $L > kx$.

Figure 2 shows the actual absolute error and the computed approximation ϵ_T when $C_1 = 1$ as a function of L. Clearly, the actual error reaches the asymptotic form (with $C_1 = 1$) when L is somewhat larger than kx.

Now we will turn to the error caused by the numerical integration. The integral appearing in (56) needs to be computed numerically. The total error from the numerical integration is

$$\epsilon_I = \left|\frac{k^2}{4\pi}\sum_{l=0}^{L}(2l+1)i^l h_l^{(1)}(kx)\epsilon_i\right|, \tag{66}$$

where ϵ_i represents the error from numerical quadrature of the integral in (56). Equations (14) and (16) show that this integral reduces essentially to

$$\int_{S_1} Y_l^m(\hat{\mathbf{s}})[Y_{l'}^{m'}(\hat{\mathbf{s}})]^* \, d\omega_s = \delta_{mm'}\delta_{ll'}. \tag{67}$$

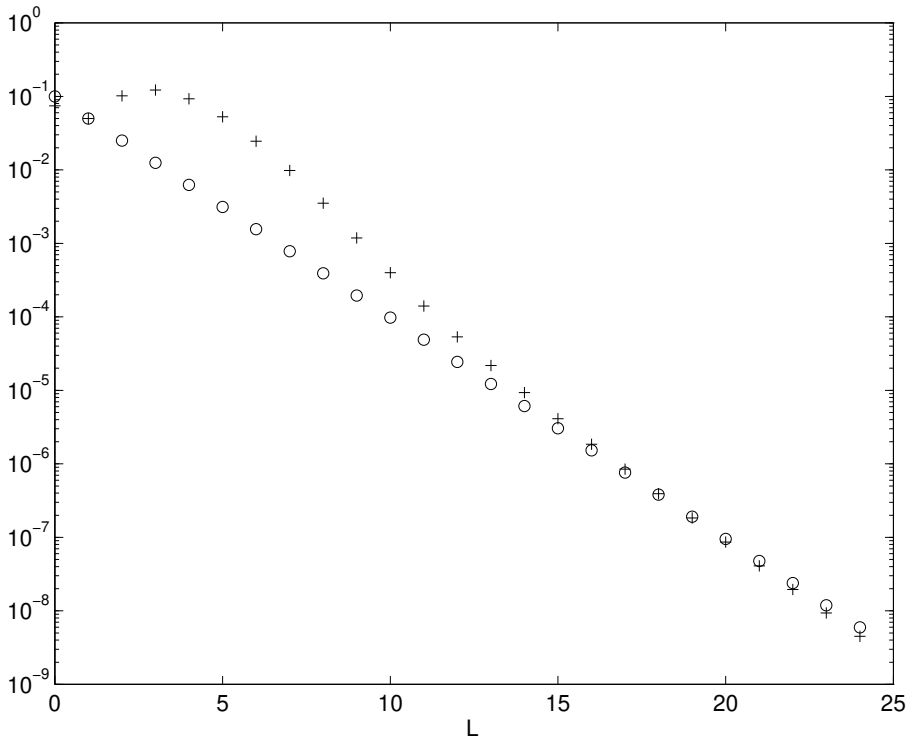

Figure 2: The actual absolute truncation error of the dipole potential in (55) (pluses) and the approximate bound ϵ_T from (65) (circles) as a function of L when $kx = 10$ and $ky = 5$.

This integral is thus implicitly computed numerically. The integration of two spherical harmonics can be separated to the product of

$$I_1 = \int_0^{2\pi} e^{i(m-m')\phi}\, d\phi \tag{68}$$

and

$$I_2 = \int_0^{\pi} P_l^m(\cos\theta) P_{l'}^{m'}(\cos\theta) \sin\theta\, d\theta. \tag{69}$$

Now we will need the following two lemmas

Lemma 2 *The integral I_1 can be computed exactly with the p_1-point trapezoidal rule if $p_1 - 1 \geq |m| + |m'|$.*

Proof. The n-point trapezoidal rule on the interval $[a, b]$ for a function g is

$$T(g, a, b, n) = h[\frac{1}{2}g(a) + g(a+h) + \ldots + g(a+(n-1)h) + \frac{1}{2}g(b)], \tag{70}$$

where $h = (b-a)/n$. If the function $g(x)$ belongs to $C^{2j+1}[a, b]$ and its derivatives up to degree $2j-1$ coincide at the end points, the Euler-Maclaurin formula gives the integration error as [7]

$$T(g, a, b, n) - \int_a^b g(x)\, dx = h^{2j+1} \int_a^b B_{2j+1}\left(n\frac{x-a}{b-a}\right) g^{(2j+1)}(x)\, dx, \tag{71}$$

where

$$B_{2j+1}(x) = (-1)^{j-1} \sum_{n'=1}^{\infty} \frac{2\sin 2\pi n' x}{(2\pi n')^{2j+1}}. \tag{72}$$

When we take $g(x) = e^{i\mu x}$, and $[a, b] = [0, 2\pi]$, the right hand side of (71) is essentially of the form

$$\int_0^{2\pi} \sum_{n'=1}^{\infty} \frac{\sin nn' x}{(2\pi n')^{2j+1}} e^{i\mu x}\, dx. \tag{73}$$

Because $\sin \nu x$ is a linear combination of $e^{i\nu x}$ and $e^{i\nu x}$, the integral vanishes if $|\mu| \neq nn'$ and does so for all n' if $n > |\mu|$. □

Lemma 3 *The integral I_2 can be computed exactly by the p_2-point Gaussian quadrature, if $m = m'$ and $2p_2 - 1 \geq l + l'$.*

Proof. By a change of variable, the integral I_2 is equivalent to

$$I_2 = \int_{-1}^{1} P_l^m(x) P_{l'}^{m'}(x)\, dx. \tag{74}$$

The associated Legendre function $P_l^m(x)$ is a polynomial of degree l in x if m is even and a polynomial of degree $(l-1)$ times $\sqrt{1-x^2}$ if m is odd. If $m = m'$, $P_l^m(x)P_{l'}^{m'}(x)$ is thus a polynomial of degree $(l+l')$ in x. It is well known that an l-degree polynomial Q_l can be integrated exactly with the $2l-1$-point Gauss-Legendre integration formula

$$\int_{-1}^{1} Q_l(x)\, dx = \sum_{i=1}^{2l-1} w_i Q_l(x_i), \tag{75}$$

where w_i and x_i are the integration weights and abscissas [7]. Thus the integral I_2 can be computed exactly by the p_2-point Gaussian quadrature if $2p_2 - 1 \geq l + l'$. □

From now on we set $p_1 = 2p$ and $p_2 = p$. Our procedure for numerical integration of a function $f(\hat{\mathbf{s}})$ on the surface of the unit sphere is [25]

$$\int_{S_1} f(\hat{\mathbf{s}})\, d\omega_s = \sum_{i=1}^{2p} \sum_{j=1}^{p} w_j \frac{\pi}{p} f(\hat{\mathbf{s}}_{ij}), \tag{76}$$

where $\hat{\mathbf{s}}_{ij} = (\sin\theta_j \cos\phi_i, \sin\theta_j \sin\phi_i, \cos\theta_j)$, $\theta_j = \arccos x_j$, $\phi_i = ((i-1)\pi)/p$, and x_j and w_j are the abscissae and weights for Gaussian quadrature. From here on we shall denote numerical integration with $2p \times p$ points by $\int^{2p\times p}$. A more efficient method for numerical quadrature on the sphere is given in [16].

In view of the two preceding lemmas, if $2p-1 \geq l+l'$, any product of two spherical harmonics can be exactly integrated numerically by the procedure described above. If we take $p > l/2$, we obtain from (16):

$$\int_{S_1}^{2p\times p} e^{i\mathbf{y}\cdot\hat{\mathbf{s}}} P_l(\hat{\mathbf{s}}\cdot\hat{\mathbf{x}})\, d\omega_s = 4\pi i^l j_l(ky) P_l(\hat{\mathbf{x}}\cdot\hat{\mathbf{y}}) + \sum_{l'=2p-l}^{\infty} (2l'+1) i^{l'} j_{l'}(ky) \int_{S_1} P_{l'}(\hat{\mathbf{s}}\cdot\hat{\mathbf{y}}) P_l(\hat{\mathbf{s}}\cdot\hat{\mathbf{x}})\, d\omega_s. \tag{77}$$

The last term is the error due to the numerical integration, ϵ_i, while the total numerical integration error is given by (66). The integral in ϵ_i is implicitly computed numerically, and for any integration rule, its absolute value is bounded by 4π. Thus

$$|\epsilon_i| \leq 4\pi \sum_{l'=2p-l}^{\infty} (2l'+1)|j_{l'}(ky)|. \tag{78}$$

By using the asymptotic behaviour of the function $j_l(x)$, we get the following bound for ϵ_i:

$$|\epsilon_i| \leq 4\pi C_2' \sum_{l'=2p-l}^{\infty} \frac{(2ky)^{l'} l'!}{(2l')!}, \tag{79}$$

where C_2' is a constant depending on ky. To compute this sum, we use the following lemma.

Lemma 4

$$\sum_{l=m}^{\infty} \frac{(2x)^l l!}{(2l)!} = \frac{\sqrt{\pi x/2}\, e^{x/2}\, \gamma(m-1/2, x/2)}{\Gamma(m-1/2)} = \frac{(2x)^m m!}{(2m)!} M(1, m+1/2, x/2), \tag{80}$$

where $\Gamma(x)$ is the gamma function, $\gamma(m,x)$ is the incomplete gamma function and $M(a,b,x)$ is the confluent hypergeometric function defined by

$$M(a,b,x) = \sum_{m=0}^{\infty} \frac{(a)_m x^m}{(b)_m m!}. \tag{81}$$

Proof. The special functions and their relations are defined in Abramowitz and Stegun [1], chapter 6 and 13. The first identity is obtained by changing the summation to start from 0 and utilizing Equations 6.5.29, 6.5.4, and 6.5.2 in [1]. The second identity follows from 6.5.12. □

When $m > x$, $M(1, m+1, x/2) \sim 1/(1-x/(2m))$ and for a fixed x, this estimate goes to unity as m grows. In the preceding lemma, $((2x)^m m!)/((2m)!)$ is approximately given by $x j_{m-1}(x)$. Thus we take $\epsilon_i \leq 4\pi C_2'' \; ky \; j_{2p-l-1}(ky)$, where C_2'' is a constant. Note that when the integral in the left hand side of (77) is computed numerically, its value does not go below the machine precision ϵ_{mach}, defined as the smallest number such that in machine arithmetic $1 + \epsilon > 1$.

Now we can state our main theorem in the dipole case. We assume that in the potential expansions $x \geq cy$, where c is a constant greater than one. The relative error ϵ_{rel} is the sum of the truncation and integration errors $\epsilon_T + \epsilon_I$ divided by the absolute value of the potential.

Theorem 2 *Let x_1 be the largest value of x occurring in the potential expansions (i.e. the largest distance between centers of computational cells), $L > kx_1$, and $x \geq cy$. For each kx_1 there exist constants C_1 and C_2 such that if the integral in (56) is computed numerically with $2L \times L$ points, the relative error for the L-point truncated expansion of the dipole potential is bounded by*

$$\epsilon_{rel} \leq C_1 \frac{1 + 1/c}{1 - 1/c} \left(\frac{1}{c}\right)^{L+1} + C_2(2L+1)(1 + \frac{1}{c}) \left(\frac{1}{c}\right)^{L}. \tag{82}$$

Proof. Combining (65), a truncated version of (56), (77), and (66) together with the estimate for ϵ_i, we obtain

$$\left| -ik \frac{e^{ik|\mathbf{x}+\mathbf{y}|}}{|\mathbf{x}+\mathbf{y}|} - \frac{k^2}{4\pi} \sum_{l=0}^{L} (2l+1) i^l h_l^{(1)}(kx) \int_{S_1}^{2p \times p} e^{ik\mathbf{y}\cdot\hat{\mathbf{s}}} P_l(\hat{\mathbf{s}} \cdot \hat{\mathbf{x}}) \, d\omega_s \right|$$

$$\leq \; C_1 \frac{k}{(x-y)} \left(\frac{y}{x}\right)^{L+1} + k^2 C_2''' \sum_{l=0}^{L} (2l+1) \, |h_l^{(1)}(kx)| \, ky \, j_{2p-l-1}(ky). \tag{83}$$

By far the dominant term in the sum is the term $l = L$. Now we set $p = L$, and use the asymptotic forms of the Bessel functions, and after some manipulations we find

$$\epsilon_{abs} \leq C_1 \frac{k}{(x-y)} \left(\frac{y}{x}\right)^{L+1} + kC_2 \frac{(2L+1)}{x} \left(\frac{y}{x}\right)^{L}. \tag{84}$$

A lower bound for the absolute value of the dipole potential is

$$\left| -ik \frac{e^{ik|\mathbf{x}+\mathbf{y}|}}{|\mathbf{x}+\mathbf{y}|} \right| \geq \frac{k}{(x+y)}. \tag{85}$$

The theorem follows by dividing ϵ_{abs} by this and using $x \geq cy$. □

The above result is based on the assumption that the left-hand side of (77) is larger than machine precision. If this fails, the decay of the function $j_l(ky)$ no more cancels the growth of $h_l^{(1)}(kx)$ resulting to a loss of accuracy. Figure 3 shows the actual absolute error and the estimate (84). The effects of finite precision arithmetic can clearly be seen.

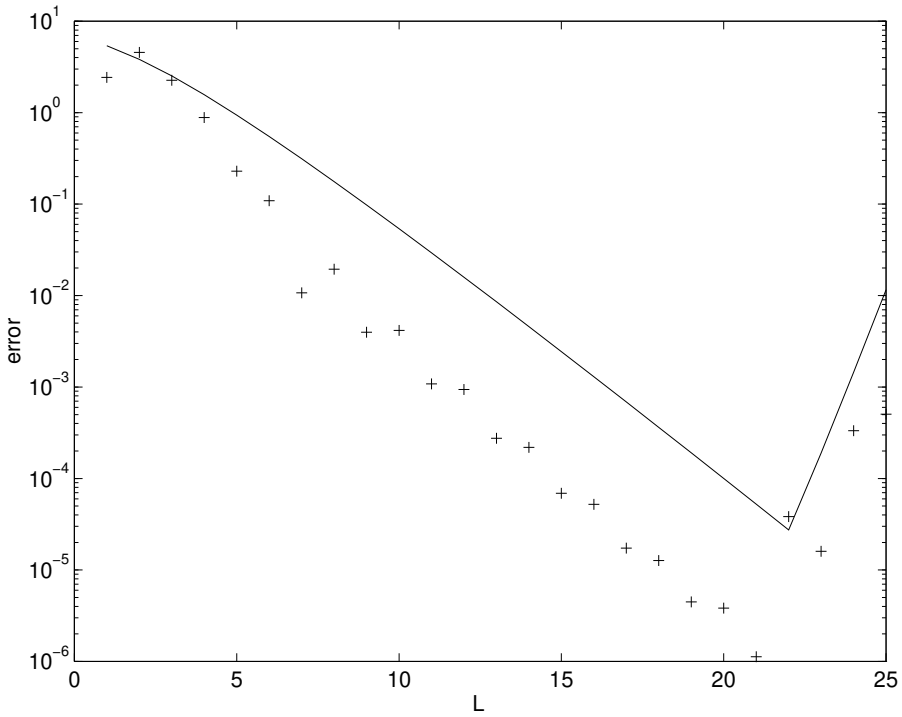

Figure 3: The actual absolute error (pluses) for the dipole potential and the error estimate (84) (solid line) when $kx = 6.4$ and $ky = 3.2$.

4.2 Error for the electric field

The error analysis for the expansion of the electric field is much more complicated than for the dipole potential, although the computation of electric field is a very slight modification of the dipole potential.

To compute the electric field from the dipole potential, we start with (56) and writing the derivatives as in (38), we obtain in dyadic notation

$$\mathbf{E}_j(\mathbf{r}) = (\nabla\nabla + k^2\mathbf{1})\frac{e^{ik|\mathbf{x}+\mathbf{y}|}}{|\mathbf{x}+\mathbf{y}|} = \frac{ik^3}{4\pi}\sum_{l=0}^{\infty}(2l+1)i^l h_l^{(1)}(kx)\int_{S_1} e^{ik\mathbf{y}\cdot\hat{\mathbf{s}}}(\mathbf{1}-\hat{\mathbf{s}}\hat{\mathbf{s}})P_l(\hat{\mathbf{s}}\cdot\hat{\mathbf{x}})\,d\omega_s. \tag{86}$$

If we use only L terms in the infinite series, the truncation error for this expansion is given by

$$\epsilon_T = \left\| \frac{ik^3}{4\pi}\sum_{l=L+1}^{\infty}(2l+1)i^l h_l^{(1)}(kx)\int_{S_1} e^{ik\mathbf{y}\cdot\hat{\mathbf{s}}}(\mathbf{1}-\hat{\mathbf{s}}\hat{\mathbf{s}})P_l(\hat{\mathbf{s}}\cdot\hat{\mathbf{x}})\,d\omega_s \right\|. \tag{87}$$

Here $\|\cdot\|$ denotes the norm of the dyad viewed as a linear operator. Using (15) we obtain

$$\epsilon_T = \left\| \frac{ik^3}{4\pi}\sum_{l=L+1}^{\infty}(2l+1)i^l h_l^{(1)}(kx)\sum_{l'=0}^{\infty}(2l'+1)i^{l'} j_{l'}(ky)\mathbf{I}(l,l') \right\|, \tag{88}$$

where

$$\mathbf{I}(l,l') = \int_{S_1} P_l(\hat{\mathbf{s}}\cdot\hat{\mathbf{x}})P_{l'}(\hat{\mathbf{s}}\cdot\hat{\mathbf{y}})(\mathbf{1}-\hat{\mathbf{s}}\hat{\mathbf{s}})\,d\omega_s \tag{89}$$

A double application of (11) gives

$$\mathbf{I}(l,l') = \frac{4\pi}{2l+1}\frac{4\pi}{2l'+1}\sum_{m=-l}^{l}\sum_{m'=-l'}^{l'}[Y_l^m(\hat{\mathbf{y}})]^* Y_{l'}^{m'}(\hat{\mathbf{x}})\,\mathbf{I}(l,l',m,m'), \tag{90}$$

where we have denoted

$$\mathbf{I}(l,l',m,m') = \int_{S_1}[Y_{l'}^{m'}(\hat{\mathbf{s}})]^* Y_l^m(\hat{\mathbf{s}})(\mathbf{1}-\hat{\mathbf{s}}\hat{\mathbf{s}})\,d\omega_s. \tag{91}$$

The terms in the tensor (or dyadic) $\hat{\mathbf{s}}\hat{\mathbf{s}}$ can be written in terms of the spherical harmonics. Indeed, in spherical coordinates, $\hat{\mathbf{s}}\hat{\mathbf{s}}$ has the form

$$\hat{\mathbf{s}}\hat{\mathbf{s}} = \begin{pmatrix} \sin^2\theta\cos^2\phi & \sin^2\theta\sin\phi\cos\phi & \sin\theta\cos\theta\cos\phi \\ \sin^2\theta\sin\phi\cos\phi & \sin^2\theta\sin^2\phi & \sin\theta\cos\theta\sin\phi \\ \sin\theta\cos\theta\cos\phi & \sin\theta\cos\theta\sin\phi & \cos^2\theta \end{pmatrix} \tag{92}$$

It can easily be seen [3] that each of these elements is a linear combination of the spherical harmonics $Y_2^\mu(\hat{\mathbf{s}})$, where $\mu = 0, \pm1, \pm2$.

Thus the integral $\mathbf{I}(l,l',m,m')$ can be reduced to integrals of three spherical harmonics of the form

$$\int_{S_1}[Y_{l'}^{m'}(\hat{\mathbf{s}})]^* Y_l^m(\hat{\mathbf{s}})Y_2^\mu(\hat{\mathbf{s}})\,d\omega_s = (-1)^m\int_{S_1} Y_{l'}^{-m'}(\hat{\mathbf{s}})Y_l^m(\hat{\mathbf{s}})Y_2^\mu(\hat{\mathbf{s}})\,d\omega_s, \tag{93}$$

where $\mu = 0, \pm 1, \pm 2$. This integral has been much studied in quantum mechanics, and the result is given in terms of the Wigner 3-j symbols $\begin{pmatrix} j_1 & j_2 & j_3 \\ m_1 & m_2 & m_3 \end{pmatrix}$ (see for example Messiah [17]):

$$\int_{S_1} Y_{j_1}^{m_1}(\hat{\mathbf{s}}) Y_{j_2}^{m_2}(\hat{\mathbf{s}}) Y_{j_3}^{m_3}(\hat{\mathbf{s}})\, d\omega_s = \sqrt{\frac{(2j_1+1)(2j_2+1)(2j_3+1)}{4\pi}} \begin{pmatrix} j_1 & j_2 & j_3 \\ 0 & 0 & 0 \end{pmatrix} \begin{pmatrix} j_1 & j_2 & j_3 \\ m_1 & m_2 & m_3 \end{pmatrix}. \tag{94}$$

The Wigner 3-j symbols are nonzero only if $|j_1 - j_2| \le j_3$, giving $|l - l'| \le 2$. The 3-j symbol $\begin{pmatrix} j_1 & j_2 & j_3 \\ 0 & 0 & 0 \end{pmatrix}$ is nonzero only if $j_1 + j_2 + j_3$ is even. Thus we have only the possibilities $l - l' = -2, 0, 2$.

In deriving a bound for the truncation error, we are only interested in the case $l' = l - 2$, as it gives the largest value in the summation (88). The norm of the tensor $\int_{S_1} P_l(\hat{\mathbf{s}} \cdot \hat{\mathbf{x}}) P_{l-2}(\hat{\mathbf{s}} \cdot \hat{\mathbf{y}})(\mathbf{1} - \hat{\mathbf{s}}\hat{\mathbf{s}})\, d\omega_s$ is bounded by 4π. (Numerical tests suggest that the integral decays like $1/l$, but we were unable to prove this.) We now obtain a bound for the truncation error of the expansion of the electric field.

Lemma 5 *When $L > kx$ and $x > y$, for each x and k there exist constants C_1' and C_1 such that when the potential expansion (86) of the electric field is truncated to L terms, the truncation error is bounded by*

$$\epsilon_T \le C_1' k^3 \sum_{l=L+1}^{\infty} (2l+1)(2l-3) |h_l^{(1)}(kx)| j_{l-2}(ky) \tag{95}$$

$$\le C_1 \frac{1}{x^2(x-y)} \left(\frac{y}{x}\right)^{L-1} (2L)^3. \tag{96}$$

Proof. The first bound follows by inserting the bound of the tensor integral into (88). Using asymptotic forms of the spherical Bessel functions,

$$\epsilon_T \le C_1'' k^3 \sum_{l=L+1}^{\infty} \frac{(2l+1)^3}{(kx)^3} \left(\frac{y}{x}\right)^{l-2}. \tag{97}$$

The last bound follows after some algebra, where terms lower than L^3 are neglected. □

Now we will consider numerical integration in conjunction with the computation of the electric field. The integral in (86) is computed numerically in the same fashion as in the case of a dipole potential. The total error from the numerical integration is

$$\epsilon_I = \left\| \frac{ik^3}{4\pi} \sum_{l=0}^{L} (2l+1) i^l h_l^{(1)}(kx) \epsilon_i, \right\|, \tag{98}$$

where ϵ_i is the error from computing the integral in (86). We implicitly compute numerically integrals of the form (91) for which we need the following lemma.

Lemma 6 *Integrals of the form*

$$\int_{S_1} Y_{l'}^{m'}(\hat{\mathbf{s}})[Y_l^m(\hat{\mathbf{s}})]^*(\mathbf{1}-\hat{\mathbf{s}}\hat{\mathbf{s}})\,d\omega_s,\ m=-l,\ldots,l,\ m'=-l',\ldots,l' \tag{99}$$

are computed exactly by the $2p$-point trapezoidal rule in the ϕ direction and by the p-point Gauss-Legendre rule in the θ direction if $2p-1 \geq l+l'+2$.

Proof. The term associated with the unit tensor has already been dealt with in the case of the dipole potential. We shall first look at the dependence on ϕ in the integral

$$\mathbf{I} = \int_{S_1} Y_{l'}^{m'}(\hat{\mathbf{s}})[Y_l^m(\hat{\mathbf{s}})]^*\hat{\mathbf{s}}\hat{\mathbf{s}}\,d\omega_s. \tag{100}$$

The dependence on ϕ in the integral (100) is clearly a sum of terms $e^{i(m'-m+\mu)}$, where $|\mu| \leq 2$. The elements of the tensor $\mathbf{I}$ associated with the elements s_{11}, s_{12}, and s_{22} of the tensor $\hat{\mathbf{s}}\hat{\mathbf{s}}$ vanish unless $m-m' = 0, \pm 2$. The same applies to s_{33} unless $m = m'$ and to s_{13} and s_{23} unless $m - m' = \pm 1$. In the nonzero components of $\mathbf{I}$ corresponding to s_{11}, s_{12}, s_{22}, or s_{33} the dependence on θ is a polynomial of degree $l+l'$ in $\cos\theta$ times $\cos^2\theta$ or $\sin^2\theta$. For the nonzero terms corresponding to s_{13} or s_{23}, the θ-dependence is a polynomial of degree $l+l'-1$ in $\cos\theta$ times $\sqrt{1-\cos^2\theta}$ times $\sin\theta\cos\theta$. Thus the dependence on θ is a polynomial of degree $l+l'+2$ in $\cos\theta$. The lemma follows by observing the bounds on m and m' and using Lemmas 2 and 3. □

Looking at the expansion (88) and using Lemma 6, the error from the integral in (86) can be bounded by

$$\epsilon_i \leq C_2'\,4\pi \sum_{l'=2p-l-2}^{\infty} (2l'+1)|j_{l'}(ky)|, \tag{101}$$

if we use $2p \times p$ integration points. The sum can be approximated by $ky\,j_{2p-l-3}(ky)$, as Lemma 4 and the discussion following it shows. Again the effects of finite machine precision have to be taken into account. We shall first give a result describing the absolute error in the dipole case. This follows after a completely similar reasoning as in the proof of Theorem 2.

Theorem 3 *When $L > kx$ and $x > y$, for each k and x there exist constants C_1 and C_2 such that if we use $2L \times L$ points in the numerical integration in (86), the absolute error for the electric field $\epsilon_{abs} = \epsilon_T + \epsilon_I$ is bounded by*

$$\epsilon_{abs} \leq C_1 \frac{8L^3}{x^2(x-y)}\left(\frac{y}{x}\right)^{L-1} + C_2\frac{8L^3}{xy^2}\left(\frac{y}{x}\right)^{L}. \tag{102}$$

A strict bound for the relative error is more difficult to find, because the absolute values of the electric field grows like $1/r^3$ near the origin and decays like $1/r$ far from the origin. The following bound is derived in the $1/r^3$ regime, where we approximate $|\mathbf{E}(\mathbf{r})| \geq 2/(x+y)^3$ and $x \geq cy$:

$$\epsilon_{rel} \leq C_1\frac{(1+1/c)^3}{1-1/c}\left(\frac{1}{c}\right)^{L-1} 4L^3 + C_2(1+1/c)^3\left(\frac{1}{c}\right)^{L-2} 4L^3. \tag{103}$$

This error bound is rather loose when kx and ky are greater than 1. The first term is probably pessimistic by a factor of L.

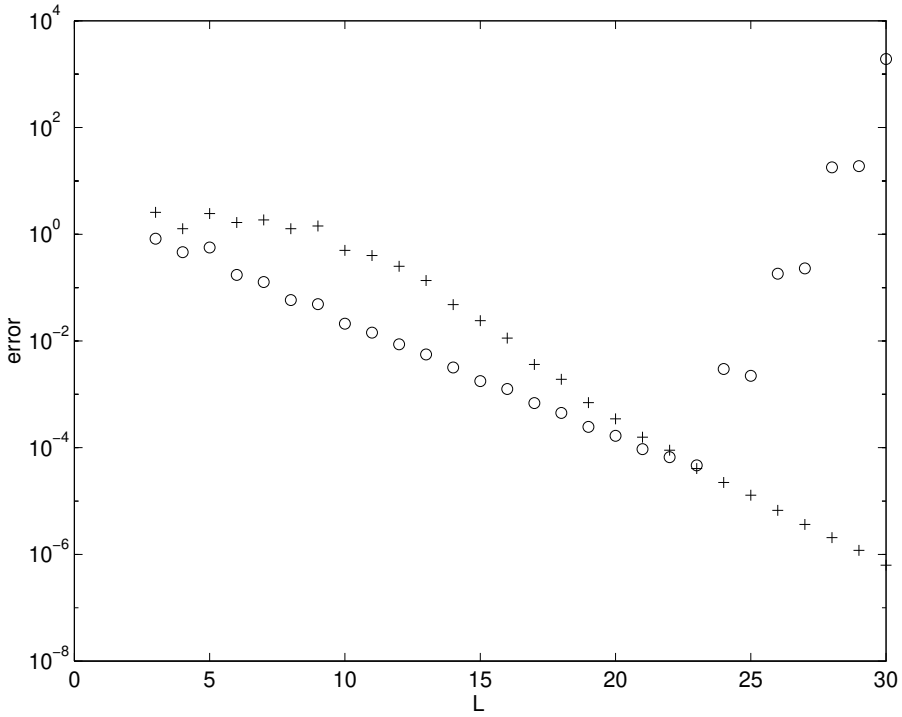

Figure 4: The actual absolute error for the electric field when $kx = 6$, $ky = 2\sqrt{3}$ (circles), and $kx = 18$, $ky = 6\sqrt{3}$ (pluses).

4.3 The impact of the error bounds

The error bounds affect the design of FMM algorithms. Especially when an adaptive FMM algorithm on many levels is employed [5, 18], the distance scales may vary greatly in magnitude. The relative error bounds are basically size-independent with two exceptions. One must use at least a number of terms proportional to the largest distances in the potential expansions. On the other hand, the growth in the spherical Bessel function $h_l^{(1)}(kx)$ is offset implicitly by the decay of the function $j_l(ky)$, but for very small distances this cancellation fails because the machine precision is reached in the numerical integration.

These effects are clearly manifested in Figure 4, which gives an example of the behaviour of the actual error of the electric field as a function of L for two cases. The ratio of x to y is the same for both cases. When $kx = 18$, the error decays linearly approximately after the point $L = kx$. When $kx = 6$, the linear rate is reached earlier, but at a certain point the effects of finite precision arithmetic destroy the decay of the error.

To reach high precision one is forced to allow the parameters p and L to vary as function of the computational level in the FMM algorithm. This means that the far-field signature functions have to be interpolated when they are used on different levels. Also the number of terms in the function $M_L(\hat{\mathbf{s}}, \mathbf{r})$ depends on the level.

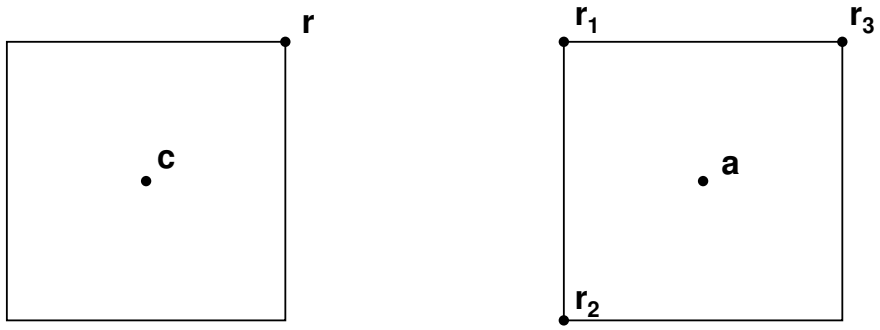

Figure 5: The multipole expansions of dipoles at positions $\mathbf{r}_1$, $\mathbf{r}_2$, and $\mathbf{r}_3$ are formed about point $\mathbf{a}$, this expansion is converted to a local expansion about point $\mathbf{c}$ and evaluated at $\mathbf{r}$. The side length of the squares are 2, giving $x = |\mathbf{c} - \mathbf{a}| = 4$, $y = |\mathbf{r} - \mathbf{c} + \mathbf{a} - \mathbf{r}_j|$, $y = 2$, $\sqrt{2}$, and 0 for points $\mathbf{r}_1$, $\mathbf{r}_2$, and $\mathbf{r}_3$, respectively.

Our error analysis looks at the whole process of forming a multipole expansion, translating it into a local expansions and finally evaluating this expansion. Previously, the error bounds for the truncated multipole and local expansions we analyzed separately in the case of the Coulomb potential [12, 19]. As an example, consider the error when the potential of dipoles at points $\mathbf{r}_1$, $\mathbf{r}_2$, and $\mathbf{r}_3$ are evaluated at $\mathbf{r}$ in Figure 5. The largest error does not occur when the potential of $\mathbf{r}_1$ is computed, as might be expected. The maximum error occurs between $\mathbf{r}$ and $\mathbf{r}_2$. The contribution from point $\mathbf{r}_3$ can be computed with no error at all.

The definitions of the near-field and the interaction set in the fast multipole method determine the value c in the error bounds. In the FMM algorithm, the near-field of a particle consists of the set of particles whose contribution to the given particle is evaluated directly, rather than via the potential expansions. When the particles are collected inside cubes, the near-field is typically either the nearest neighbours or the second nearest neighbours of the cube where particle lies. The interaction set of a cube is defined by those cubes that are children of the cubes in the given cube's parent's near-field excluding the cubes that belong to the near-field of the cube itself. Examples of the near-fields and interaction sets are given in Figure 6.

In deriving the error bounds, we assumed that $x > cy$. The value of c depends on the choice of the near-field. If the near-field includes the nearest neighbours only, then we have $c = 2/\sqrt{3} \approx 1.154$. If we include the second nearest neighbours, we get $c = \sqrt{3} \approx 1.73$. Finally, the interaction set described in [18] implies $c = \sqrt{17}/3 \approx 1.374$. Thus it would seem that only the use of second nearest neighbours would guarantee a rapid convergence of the multipole expansion.

The error bounds contain unspecified constants, e.g. C_1 and C_2. These appear because of the complicated asymptotic behaviour of the spherical Bessel functions and they depend in general on kx. When the number of terms in the expansion (L) and the precision of numerical integration (p) is much larger than kx, the constants can be replaced with unity.

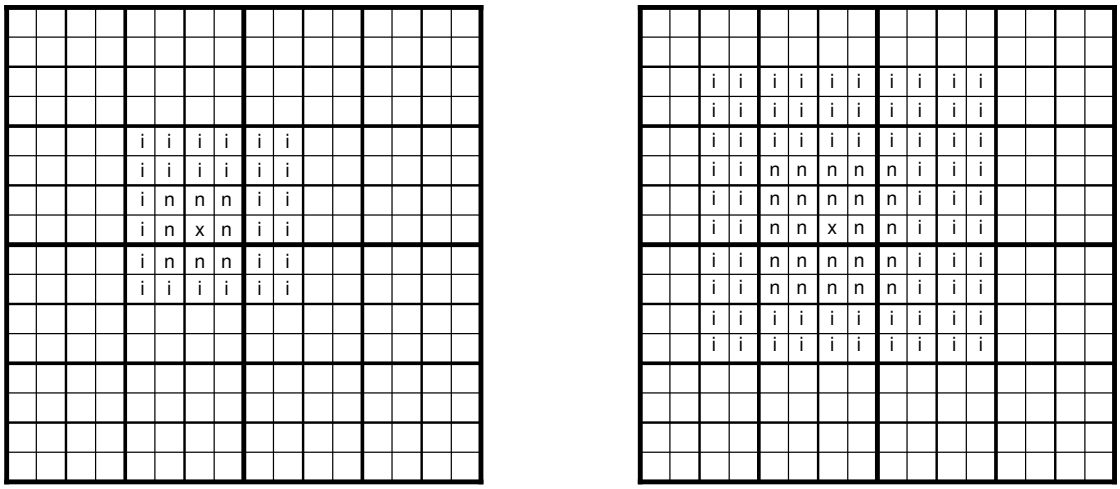

Figure 6: Two examples of the near-fields (n) and interaction sets (i) of a particle (x). In the left figure, the near-field consists of the nearest neighbours of the particle, in the right figure it contains the second nearest neighbours.

5 Conclusion

A simplified derivation of the diagonal forms of the translation operators for the Helmholtz equation is given. These operators are needed when either the scalar or vector Helmholtz equation (acoustic or electromagnetic scattering) is solved using integral equation techniques, the resulting system of linear equations is solved with iterative methods, and the matrix-vector products are computed with the fast multipole method.

The diagonal forms of the translation operators are based on truncated series expansions of the potentials. The diagonal forms are obtained using certain integral representations while the potentials are recovered using numerical integration on the surface of the unit sphere. We are essentially using Fourier transformed quantities. The standard translation operators for the potential expansions are expressed as convolutions [9], and in the Fourier space these can be replaced with pointwise multiplication, giving the diagonal forms. Moreover, going from the potential of a dipole to the electric field requires differentiation which can be expressed as multiplication by the transform variable in the Fourier space.

We present error analysis of the FMM algorithm for the Helmholtz equation. There are two sources for errors, truncation of the infinite series expansions, and numerical integration. The error analysis is fairly complicated because the magnitudes of the Bessel functions are hard to estimate when both the order and the argument of the Bessel functions are large. Finally, the implications of the error bounds on the FMM algorithm are discussed.

6 Acknowledgement

I am grateful to professor Olavi Nevanlinna, Olli Serimaa, and my wife Satu for their comments on the manuscript. I thank Olavi Nevanlinna for the fruitful discussions we have had on this subject. Olli Serimaa has given valuable advice on the use of special functions and potential expansions. The Center for Scientific Computing has provided the computer time for the experiments. This work has been financially supported by the Jenny and Antti Wihuri foundation.

References

[1] M. Abramowitz and I. A. Stegun, editors. *Handbook of mathematical functions with formulas, graphs, and mathematical tables.* Wiley, New York, 1972.

[2] C. R. Anderson. An implementation of the fast multipole method without multipoles. *SIAM J. Sci. Stat. Comput.*, 13:923–947, 1992.

[3] G. Arfken. *Mathematical Methods for Physicists.* Academic Press, Orlando, Florida, 3. edition, 1985.

[4] L. P. Bayvel and A. R. Jones. *Electromagnetic scattering and its applications.* Applied Science Publishers, London, 1981.

[5] J. Carrier, L. Greengard, and V. Rokhlin. A fast adaptive multipole algorithm for particle simulations. *SIAM J. Sci. Stat. Comput.*, 9:669–686, 1988.

[6] R. Coifman, V. Rokhlin, and S. Wandzura. The fast multipole method for the wave equation: a pedestrian prescription. *IEEE Antennas and Propagation Magazine*, 35(3):7–12, June 1993.

[7] P. J. Davis and P. Rabinowitz. *Methods of Numerical Integration.* Academic Press, New York, 1975.

[8] N. Engheta, W. D. Murphy, V. Rokhlin, and M. S. Vassiliou. The fast multipole method (FMM) for electromagnetic scattering problems. *IEEE Trans. on Antennas and Propagation*, 40:634–641, 1992.

[9] M. A. Epton and B. Dembart. Multipole translation theory for the 3-D Laplace and Helmholtz equations. *SIAM J. Sci. Comput.*, 16(4), 1995.

[10] R. W. Freund. Conjugate gradient-type methods for linear systems with complex symmetric coefficient matrices. *SIAM J. Sci. Stat. Comput.*, 13:425–448, 1992.

[11] J. W. Gibbs. Elements of vector analysis. In *The Scientific Papers of J. Willard Gibbs.* Dover, New York, 1961. Original edition printed privately, New Haven 1884.

[12] L. Greengard and V. Rokhlin. A fast algorithm for particle simulations. *J. Comp. Phys.*, 73:325–348, 1987.

[13] J. D. Jackson. *Classical Electrodynamics*. Wiley, New York, 1983.

[14] I. V. Lindell. *Methods for electromagnetic field analysis*. Oxford University Press, Oxford, 1992.

[15] K. Lumme and J. Rahola. Light scattering by porous dust particles in the discrete-dipole approximation. *Astrophys. J.*, 425:653–667, 1994.

[16] A. D. McLaren. Optimal numerical integration on a sphere. *Math. Comput.*, 17, 1963.

[17] A. Messiah. *Quantum Mechanics*. North-Holland, Amsterdam, 1961.

[18] K. Nabors, F. T. Korsmeyer, F. T. Leighton, and J. White. Preconditioned, adaptive, multipole-accelerated iterative methods for three-dimensional first-kind integral equations of potential theory. *SIAM J. Sci. Comp.*, 15:713–735, 1994.

[19] G. J. Pringle. *Numerical Study of Three-Dimensional Flow using Fast Particle Algorithms*. PhD thesis, Napier University, Edinburgh, 1994.

[20] E. M. Purcell and C. R. Pennypacker. Scattering and absorption of light by nonspherical dielectric grains. *Astrophys. J.*, 186:705–714, 1973.

[21] J. Rahola. Solution of dense systems of linear equations in electromagnetic scattering calculations. Licenciate's thesis, Helsinki University of Technology, 1994.

[22] J. Rahola. Solution of dense systems of linear equations in the discrete-dipole approximation. CSC Preprint Series 1/1994, Center for Scientific Computing, 1994. To appear in SIAM J. Sci. Comput.

[23] V. Rokhlin. Rapid solution of integral equations of classical potential theory. *J. Comp. Phys.*, 60:187–207, 1985.

[24] V. Rokhlin. Rapid solution of integral equations of scattering theory in two dimensions. *J. Comp. Phys.*, 86:414–439, 1990.

[25] V. Rokhlin. Diagonal forms of translation operators for the Helmholtz equation in three dimensions. *Applied and Computational Harmonic Analysis*, 1:82–93, 1993.

[26] P. Zwamborn and P. M. van der Berg. Computation of electromagnetic fields inside strongly inhomogeneous objects by the weak-conjugate-gradient fast-Fourier-transform method. *J. Opt. Soc. Am. A*, 11:1414–1421, 1994.